Contribution 6.10.2
Tunneling control and localization for Bose-Einstein condensates in a frequency modulated optical lattice

A. Zenesini[1],* H. Lignier[2],† C. Sias[2],‡ O. Morsch[2], D. Ciampini[1,2], and E. Arimondo[1,2§]
[1] *Dipartimento di Fisica E.Fermi, Università di Pisa, Largo Pontecorvo 3, 56127 Pisa, Italy*
[1] *CNISM, Unitá di Pisa, Dipartimento di Fisica E.Fermi Largo Pontecorvo 3, 56127 Pisa, Italy and*
[2] *CNR-INFM, Dipartimento di Fisica E.Fermi, Università di Pisa, Lgo Pontecorvo 3, I-56127 Pisa,Italy*
(Dated: July 31, 2018)

The similarity between matter waves in periodic potential and solid-state physics processes has triggered the interest in quantum simulation using Bose-Fermi ultracold gases in optical lattices. The present work evidences the similarity between electrons moving under the application of oscillating electromagnetic fields and matter waves experiencing an optical lattice modulated by a frequency difference, equivalent to a spatially shaken periodic potential. We demonstrate that the tunneling properties of a Bose-Einstein condensate in shaken periodic potentials can be precisely controlled. We take additional crucial steps towards future applications of this method by proving that the strong shaking of the optical lattice preserves the coherence of the matter wavefunction and that the shaking parameters can be changed adiabatically, even in the presence of interactions. We induce reversibly the quantum phase transition to the Mott insulator in a driven periodic potential.

PACS numbers:

I. INTRODUCTION

Since the early days of quantum mechanics toy models have been used to explain and teach the counterintuitive phenomena of the quantum world. The possibility to solve analytically a number of simple problems showed how complex processes were related to basics ideas. The particle in the box or the potential barrier are only two examples. Till the end of the last century, however, it was almost impossible to realize these simple toy models because of the temperature and energy scale required to perform such experimental investigations. The single quantum object under investigation was not sufficiently decoupled from the external world and decoherence processes strongly modified the quantum evolution. The experimental realization of quantum degenerate states with ultracold atomic gases allowed access to few body systems isolated from external perturbations and operating at temperatures close to absolute zero. These techniques allowed the realization of a variety of experiments testing peculiar properties of quantum mechanics. For instance, astounding examples were achieved in the study of quantum tunneling in the periodic potential associated to optical lattices [1, 2], making good use of the excellent control on all parameters of the optical lattice defect-free potential.

An important topic not extensively investigated so far is that of strongly driven quantum systems, where a time dependent (in particular periodic) perturbation is introduced in the system in order to change its properties. The external driving of a parameter of the unperturbed system produces a modification described through an effective potential similar to the rescaling of the mass for the electron motion inside a crystal. That potential contains a new variable allowing an easy understanding of the system evolution. In addition, the parameter tuning provides a new handle on the control of the quantum evolution.

This paper presents experimental results for the modification of quantum tunneling in a Bose-Einstein condensate (BEC) using a modulated frequency/phase difference of the optical lattice potential. By periodically backwards and forwards moving the spatial position of the optical lattice minima/maxima, the tunneling properties of the atoms inside the lattice can be adiabatically changed and the atomic response is described through a rescaling of the tunneling rate. In addition, the ultracold atoms may be carried into novel regimes impossible to reach through adiabatic modifications of the Hamiltonian parameters. The tunneling rescaling applies to a macroscopic atomic ensemble, referred to as a dressed matter wave in [3]. We will show how matter waves can be adiabatically dressed without losing the quantum coherence of the ensemble, also while performing a quantum phase transition to the Mott insulator. Our experimental realization investigates simple quantum-mechanical processes in the driven regime and represents a quantum simulation of a system that is very complex to be solved analytically or numerically.

The tunneling rescaling is familiar from periodically driven single-particle quantum systems. It occurs, among others, when a particle moves on a periodically forced 1D lattice with nearest neighbor coupling such as excitons in

*Present affiliation: Physics Department, University of Innsbruck, Innsbruck, Austria.
†Present affiliation: Laboratoire Aimé Cotton, Université Paris Sud, Orsay, France.
‡Present affiliation: Cavendish Laboratory, University of Cambridge, Cambridge, UK.
§Electronic address: arimondo@df.unipi.it

an insulating crystal [4] or electrons in a semiconductor superlattice [5, 6, 7]. It also underlies the coherent destruction of tunneling of a particle in a periodically forced double well [8, 9], recently observed for argon atoms in an atomic beam [10]. Ref. [11] pointed out that coherent destruction of tunneling and dynamical localization can be interpreted as a result of destructive interference in repeated Landau-Zener crossings, and in this aspect these phenomena are similar. However, in the coherent destruction of tunneling, the initial distribution is frozen, while in the dynamical localization the distribution oscillates periodically around the initial value, even if with a small amplitude. The tunneling rescaling is completely analogous to the zero order Bessel function rescaling of atomic g factors in the presence of oscillating magnetic fields [12] examined for atoms in [13] and for BEC in [14]. The suppression of the Bloch band by the dynamical localization was observed by Raizen group [15] for cold sodium atoms in an optical lattice when a weak spectroscopy probe drove transitions between the energy bands modified by the localization process. For a BEC in a periodically shaken harmonic trap, the dynamic splitting of the condensate, and the dynamic stabilization against escape from the trap were numerically studied in [16]. A dynamical localization-like phenomenon occurs for the light propagation in two coupled optical waveguides, as predicted in [17] and observed in [18, 19]. Nonlinear dynamical localization of matter wave solitons by means of a spatial modulation of the nonlinearity changing the scattering length by means of Feshbach resonances and in the presence of optical lattice modulation was recently predicted in [20].

Section 2 introduces the concept of a shaken optical lattice. Section 3 discusses the experimental set-up, emphasizing the different techniques applied to produce the lattice shaking. Section 4 treats quantum mechanically the tunneling suppression in periodically driven systems for two different time dependences of the shaking force. Section 5 defines basic quantities characterizing ultracold gases within optical lattices. Section 6 introduces the Bose-Hubbard Hamiltonian for ultracold atoms in the presence of tunneling rescaling. Section 7 reports the experimental results of [21, 22] on the tunneling rescaling in strongly driven one-dimensional quantum systems and on the rescaling applied to produce a Mott insulator.

II. SHAKEN OPTICAL LATTICE

In a 1D optical lattice a standing wave is created by the interference of two linearly polarized traveling waves counter-propagating along the x axis with frequency $\omega_{\rm L}$ and wavevector $k_{\rm L}$ [2, 23]. The amplitude of the generated electric field is $\mathcal{E}(r,t) = 2\mathcal{E}_0 sin(\omega_{\rm L} t) sin(k_{\rm L} x)$. When the laser detuning from the atomic transition is large enough to neglect the excited state spontaneous emission decay, the atom experiences a periodically varying conservative potential

$$V_{\rm ol}(x) = \frac{V_0}{2} cos(2k_{\rm L} x). \tag{1}$$

The amplitude V_0 depends on the laser detuning from the atomic transition and on the standing wave laser intensity [24]. The periodic potential has a $d_{\rm L} = \pi/k_{\rm L}$ spacing. This potential derives from the quantum mechanical interaction between atom and optical lattice photons. Therefore the lattice quantities are linked to the recoil momentum $p_{\rm rec} = \hbar k_{\rm L}$ acquired by an atom after the absortion or the emission of one photon. V_0 will be expressed in units of $E_{\rm rec}$ the recoil energy acquired by an atom having mass M following one photon exchange

$$E_{\rm rec} = \frac{\hbar^2 k_{\rm L}^2}{2M}. \tag{2}$$

We now introduce a periodic driving (often referred to as shaking in the following) to the system of atoms inside the optical lattice. In the lattice reference frame a backwards and forwards motion of the periodic potential at frequency ω along one direction is equivalent to a periodic force $Fcos(\omega t)$ applied to the atoms and to the following potential:

$$V_{\rm sh}(t) = K cos(\omega t) \sum_{\rm m} m|m><m|. \tag{3}$$

Here $K = F d_{\rm L}$, the modulation amplitude, is the energy difference between neighboring sites of the linear chain and $|m>$ denotes the the localized Wannier wavefunction of an atom in the site m of the optical lattice [25, 26]. The theoretical analysis of Sec. IV evidences the key role of the dimensionless parameter K_0 defined by

$$K_0 = \frac{K}{\hbar\omega}. \tag{4}$$

III. SET-UP

A. BEC and optical lattices

We created BEC's of ^{87}Rb atoms using a hybrid approach in which evaporative cooling was initially effected in a magnetic time-orbiting potential trap and subsequently in a crossed dipole trap. The dipole trap was realized by using two intersecting Gaussian laser beams at 1030 nm wavelength and a power of around 1 W per beam focused to waists of 50 μm. After obtaining pure condensates of about 5×10^4 atoms, the powers of the trap beams were adjusted in order to obtain condensates with the desired trap frequencies in the longitudinal and radial directions. Subsequently, the BECs held in the dipole trap were loaded into 1D or 3D optical lattice created by counterpropagating Gaussian laser beams at 842 nm with 120 μm waists and a resulting optical lattice spacing $d_{\rm L}$= 421 nm. The optical lattice laser beams were ramped up

in power in about 50 ms, this ramping time being chosen so as to avoid excitations of the BEC. By introducing a frequency difference $\Delta\nu$ between two counterpropagating lattice beams (using the acousto-optic modulators which also control the power of the beams), the optical lattice could be moved at a velocity $v_{\rm L} = d_{\rm L}\Delta\nu$ along the propagation direction of those laser beams. In addition the optical lattice could be accelerated (or decelarated) with an acceleration $a_{\rm L} = d_{\rm L}\frac{\delta}{\delta t}\Delta\nu$, leading to a force $F = Ma_{\rm L}$ in the rest frame of the lattice.

B. Shaking set-up

The shaking of the optical lattices was realized through two different schemes, described in the following.

1) Modulated frequency difference. In this configuration the optical lattice is created by two independent laser beams counter-propagating along one direction. The beams experience separate frequency modulations in the passage trough two separate acousto-optic modulators (AOM). Each AOM is driven by a function generator whose frequency can be modulated both with internal preset functions or by using a triggered external channel. The optical lattice shaking amplitude is related to the modulation amplitude $\Delta\nu$ for the frequency offset between the two laser beams. For the case of a sinusoidal modulation $\Delta\nu_{\rm max}sin(\omega t)$ we have

$$\begin{aligned} F(t) &= F_{\rm max}cos(\omega t) = Md_{\rm L}\frac{d}{dt}\left[\Delta\nu_{\rm max}sin(\omega t)\right] \\ &= Md_{\rm L}\omega\Delta\nu_{\rm max}cos(\omega t), \end{aligned} \tag{5}$$

leading to

$$K_0 = \frac{Md_{\rm L}^2\omega\Delta\nu_{\rm max}}{\hbar\omega} = \frac{\pi^2}{2}\frac{\Delta\nu_{\rm max}}{\omega_{\rm rec}}. \tag{6}$$

2) Modulated phase difference. In this case one of the optical lattice beams is created by retro-reflecting a laser beam on a mirror mounted on a piezoelectric actuator. The piezo-electric actuator is driven by a function generator, and the expansion of the device is proportional to the voltage applied to it. For a displacement $\Delta x_{\rm max}cos(\omega t)$ of the mirror, we obtain

$$K_0 = \frac{M\omega^2\Delta x_{\rm max}d_{\rm L}}{\hbar\omega} = \frac{\pi^2}{2}\frac{\omega}{\omega_{\rm rec}}\frac{\Delta x_{\rm max}}{d_{\rm L}}. \tag{7}$$

IV. DYNAMIC LOCALIZATION

The atomic evolution in the shaken optical lattice may be studied by considering the localized Wannier wavefunction $|m>$ and the perturbations originating from the atomic occupation in neighboring sites [25, 26]. This approximation is valid when the overlap of atomic wavefunctions introduces corrections to the localized atom picture, but they are not large enough to render the single site description irrelevant. We write for the atomic Hamiltonian H

$$\begin{aligned} H &= E_0\sum_m |m><m| \\ &- J\sum_m \left(|m><m+1| + |m+1><m|\right). \end{aligned} \tag{8}$$

For ultracold atoms in an optical lattice of depth V_0 the nearest-neighbor tunneling enery J is given by [27]

$$J = \frac{4}{\sqrt{\pi}}E_{\rm rec}\left(\frac{V_0}{E_{\rm rec}}\right)^{3/4} exp\left(-2\sqrt{\frac{V_0}{E_{\rm rec}}}\right) \tag{9}$$

The generic atomic wave function can be written as a superposition of the $|m>$ localized wavefunctions

$$|\Psi(x)> = \sum_m C_{\rm m}|m>. \tag{10}$$

The temporal evolution for the $C_{\rm m}$ coefficients under the H Hamiltonian is given by

$$i\hbar\frac{dC_{\rm m}}{dt} = E_0C_{\rm m} + J\left(C_{\rm m+1} + C_{\rm m-1}\right), \tag{11}$$

and in the following the ground state energy E_0 will be supposed equal to zero.

Dynamic localization was introduced by Dunlap and Kenkre [5] for the motion of a charged particle in the presence of an oscillating force, created by an electric field in the original formulation. It is based on exact calculations for the evolution on a discrete lattice and is valid for a generic motion within a spatial periodic potential. The Hamiltonian for the atomic motion on the linear chain with infinite sites experiencing the periodic potential of Eq. (3) is

$$\begin{aligned} H_{\rm dyn.loc.} &= -J\sum_m \left(|m><m+1| + |m+1><m|\right) \\ &+ Kcos\left(\omega t\right)\sum_m |m><m|. \end{aligned} \tag{12}$$

For the interaction with the oscillating force $Fcos(\omega t)$ the position operator x was assumed to be diagonal in the Wannier basis [28], i.e., we have assumed

$$\int_{-\infty}^{\infty} dx < m|x><x|Fx|x><x|n> = Fd_{\rm L}m\delta_{\rm m,n}. \tag{13}$$

The evolution of the wavefunction of Eq. (10) under $H_{\rm dyn.loc.}$ produces for $C_{\rm m}$ the following equations:

$$i\hbar\frac{dC_{\rm m}}{dt} = J\left(C_{\rm m+1} + C_{\rm m-1}\right) + Kcos\left(\omega t\right)C_{\rm m}. \tag{14}$$

The solution of these coupled equations with $t = 0$ initial condition of atomic occupation of the $m = 0$ site, i.e., $C_{\rm m}(t = 0) = \delta_{\rm m=0}$ leads to [5]

$$|C_{\rm m}(t)|^2 = \mathcal{J}_{\rm m}^2\left(2Jt\left[\mathcal{J}_0^2(K_0 + \mathcal{J}_0(K_0)f_1(t) + f_2(t))\right]^{1/2}\right), \tag{15}$$

with the K_0 parameter defined in Eq. (6) and having introduced the first order Bessel function $\mathcal{J}_{\rm m}$ of the $m-$th order. The corresponding atomic mean-square displacement is

$$\frac{\sqrt{< m^2 >}}{d_{\rm L}} = \sqrt{2} Jt \left[\mathcal{J}_0^2 (K_0 + \mathcal{J}_0(K_0) f_1(t) + f_2(t))\right]^{1/2}. \tag{16}$$

Here

$$\begin{aligned} f_1(t) &= 2\frac{A_{\rm u}}{t}, \\ f_2(t) &= \frac{(A_{\rm u} + A_{\rm v})^2}{t^2}, \\ A_{\rm u}(t) &= \frac{1}{\omega}\int_0^{\omega t} cos[K_0 sin(\omega\tau)]d\tau - t\mathcal{J}_0(K_0), \\ A_{\rm v}(t) &= \frac{1}{\omega}\int_0^{\omega t} sin[K_0 sin(\omega\tau)]d\tau. \end{aligned} \tag{17}$$

The functions $f_1(t)$ and $f_2(t)$ contain the bounded functions $A_{\rm u}$ and $A_{\rm v}$ and therefore decay at large times. The expression for the $|C_{\rm m}(t)|^2$ occupation and the mean-square displacement are thus dominated by first term, unless $\mathcal{J}_{\rm m}(K_0)$ equals zero. At times $t >> 1/\omega$ the resulting simplified expressions of Eqs. (15,16) are

$$|C_{\rm m}(t)|^2 = \mathcal{J}_{\rm m}^2 (2J_{\rm eff} t), \tag{18a}$$

$$\sqrt{< m^2 >} = \frac{\sqrt{2}}{\hbar} J_{\rm eff} t, \tag{18b}$$

where we introduced the effective tunneling rate

$$J_{\rm eff} = J\mathcal{J}_0(K_0) \tag{19}$$

The applied sinusoidal force thus reduces the effective velocity of delocalization of the initially localized atom. Eq. (19) shows that the effective tunneling energy vanishes entirely whenever K_0 is a root of the $\mathcal{J}_0$ Bessel function. The remarkable result is that, then, the $m = 0$ occupation probability oscillates at frequency ω without decaying and that the mean-square displacement remains bounded. The particle is effectively localized *dynamically* by the action of the time-dependent force.

The phenomenon of dynamic localization is shown in Fig. 1 in the case of time $t = 0$ occupation of the $m = 0$ site. The temporal dependence of the $m = 0$ site is presented in (a) for $K_0 = 0$ and $K_0 = 2.405$. At $K = 0$ the decay of $|C_0|^2$ indicates the atomic escape owing to the quantum tunneling. In the special case of the roots of the $\mathcal{J}$, Bessel function the periodic recurrences of $|C_0(t = n2\pi/\omega)|^2$, with n an integer, indicates that the atom returns repeatedly to the initially occupied site. This dynamic localization is also evident from Fig 1(b) where the mean displacement for the Bessel function roots is seen to be bounded by $d_{\rm L}(2\pi|J|/\omega)$ [5].

The modification of the tunneling rate of Eq. (19) appears also in Bloch periodic wavefunctions, the alternative description for the quantum mechanical evolution within a periodic potential [25, 26]. The Bloch states

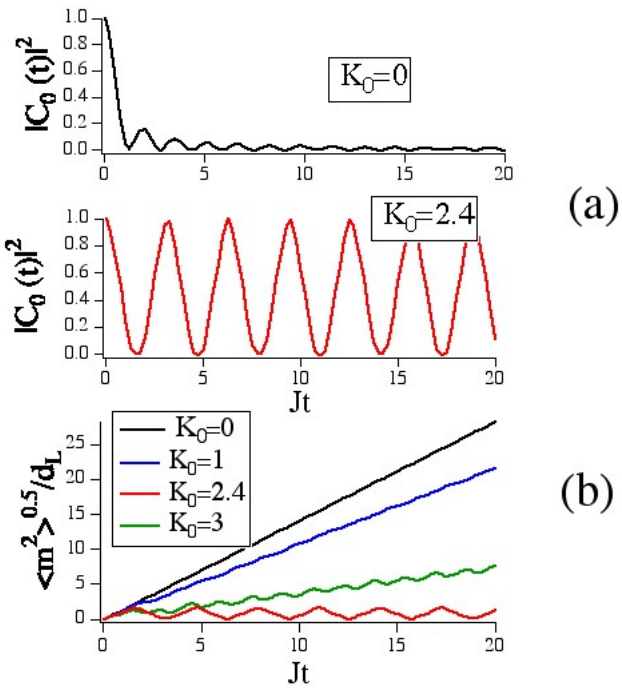

FIG. 1: In (a) the temporal dependence of $|C_0|^2$ plotted versus Jt, for $K_0 = 0$ on the top and $K_0 = 2.405$ on the bottom. For K_0 equal to a root of the Bessel function, the probability of returning to the initially occupied site reaches unity periodically with the force oscillation. In (b) dynamic localization exhibited through a plot of the mean-square displacement $\sqrt{< m^2 >}$ versus Jt for different values of K_0. It is only when K_0 is a root of $\mathcal{J}_0$ that the displacement remains bounded in time. The ratio $\hbar\omega/J = 2$ in all cases.

are energy eigenfunctions of an Hamiltonian composed by the kinetic energy and the periodic potential of Eq. (1) and are characterized by the band index n and the quasi wavenumber q. For a lattice with inversion symmetry, with coefficients given by matrix elements between Wannier states located one site apart from each other, as in Eq. (8), the $E_{\rm n=1}(q)$ energy dispersion takes the form

$$E_{\rm n=1}(q) = E_0 + 2Jcos\left(\frac{q}{k_{\rm L}}\right). \tag{20}$$

V. ULTRACOLD ATOMS

For a system of ultracold atoms in a 1D optical lattice the Bose-Hubbard model, based on the tight-binding-like approximation [29], considers interaction energies in a single site that are smaller than the gap between the ground state and the first excited level. While the model is usually based on the many body Hamiltonian with boson creation and annihilation operators at the single lattice site, for our analysis we write an Hamiltonian based

on the formalism of Eq. (12)

$$H_{\rm BH} = -J\sum_m \left(|m><m+1| + |m+1><m|\right) + U\sum_m n_{\rm m}(n_{\rm m}-1). \quad (21)$$

Here the first sum is over nearest neighboring sites (whose number is determined by the one, two or three dimension geometry), and $n_{\rm m}$ is the number operator that counts the number of atoms at the m-th site. Notice that this approach cannot be applied to describe the Mott insulator dynamic for which the second quantization approach is required. The dynamics of cold atoms in deep lattices is expressed in the Bose-Hubbard model by using only two parameters: the tunneling energy J and the on-site energy U of two atoms occupying the same lattice site, i.e. the energy required for the presence of more than one particle per site. By using simple approximations on the wavefunction [27], the dependence of U on the lattice depth V_0 may be calculated. In the 1D experimental realization it is necessary to consider the orthogonal directions along which the lattice is not present. The energy contribution to the system can be evaluated by writing the wavefunction for the transverse directions as in the weak harmonic potential that in our case is due to the dipolar trap confinement of the cloud. The 1D parameter U becomes

$$U = \frac{8}{\sqrt{\pi}} k a_{\rm s} E_{\rm rec} \left(\frac{V_0}{E_{\rm rec}}\right)^{1/4} \frac{\hbar\sqrt{\omega_{\rm y}\omega_{\rm z}}}{E_{\rm rec}}, \quad (22)$$

where $a_{\rm s}$ is the atomic scattering length and $\omega_{\rm y,z}$ are the harmonic trap frequencies in the transverse directions. In 3D optical lattice with compression applied by the light in all directions, U becomes

$$U = \frac{8}{\sqrt{\pi}} k a_{\rm s} E_{\rm rec} \left(\frac{V_0}{E_{\rm rec}}\right)^{3/4}. \quad (23)$$

VI. BOSONS IN PERIODICALLY DRIVEN OPTICAL POTENTIAL

We now add a periodic driving to the Bose-Hubbard model, with the atomic motion described by the Hamiltonian

$$\begin{aligned} H &= H_{\rm BH} + K cos(\omega t)\sum_{\rm m} m|m><m| \\ &= -J\sum_m \left(|m><m+1| + |m+1><m|\right) \\ &+ U\sum_m n_{\rm m}(n_{\rm m}-1) \\ &+ K cos(\omega t)\sum_{\rm m} m|m><m|. \end{aligned} \quad (24)$$

The full Hamiltonian is now periodic in time with period $T = 2\pi/\omega$ and a good strategy for this theoretical problem is to use the Floquet theory [30], or the dressed atom theory [12]. The solution of the Schrödinger equation with the Hamiltonian of Eq. (24) has solutions of the form

$$|\psi_{\rm n}(t) = |u_{\rm n}(t)> e^{-i\frac{\epsilon_{\rm n} t}{\hbar}} \quad (25)$$

where the so-called Floquet mode $|u_{\rm n}(t)>=|u_{\rm n}(t+T)>$ is again periodic in time with period T. The energy $\epsilon_{\rm n}$ is called a quasienergy because of the formal analogy with the quasimomentum in the Bloch problem in a spatially periodic Hamiltonian. By substituting the Floquet solution of Eq. (25) into the Schrodinger equation one arrives at an eigenvalue problem [3, 31]. Notice that the $|u_{\rm (n,0)}(t)>$ is a solution of that problem with eigenvalue $\epsilon_{\rm n}$, while then $|u_{\rm (n,m)}(t)>=|u_{\rm (n,0)}(t)> exp(im\omega t)$ is also a solution with eigenvalue $\epsilon_{\rm n} + m\hbar\omega$, where m is any positive or negative integer. At times $t = t_0 + sT$ with integer s, they all coincide, apart from a phase factor. Hence the Floquet spectrum repeats itself periodically on the energy axis. Each quasi-energy band of width $\hbar\omega$ contains one representative, labeled by m, of the class of eigenvalues belonging to the Floquet state labeled by n.

Ref. [32, 33] demonstrated that the presence of a driving force corresponds to the following renormalization of the Bose-Hubbard Hamiltonian:

$$H_{\rm ren} = -J_{\rm eff}\sum_m \left(|m><m+1| + |m+1><m|\right) + U\sum_m n_{\rm m}(n_{\rm m}-1). \quad (26)$$

where the tunneling rate J is substituted by the effective tunneling rate $J_{\rm eff}$ defined in Eq. (19) and the interaction energy U is not modified by the shaking.

This renormalized description applies also to the case when an additional static force is applied to the atoms, (theory in [34] and experimental realizations in [35, 36]).

VII. EXPERIMENTAL RESULTS

In a preliminary experiment without shaking ($K_0 = 0$), we verified that, for our expansion times, the growth in the condensate width σ along the 1D lattice direction was to a good approximation linear and for $\sigma/d_{\rm L}$ in very good agreement with the theoretical dependence of Eq. (18b) with the tunneling given by Eq. (9). Experimental results for σ versus the expansion time t at a given depth of the optical lattice are plotted in the bottom part of Fig. 2(a), and an image of the expanded condensate cloud at $t = 150$ ms is reported in Fig. 2(b). This enabled us to confirm that $d\sigma/dt$ measured at a fixed time was directly related to J and, in a shaken lattice, to $|J_{\rm eff}(K_0)|$. The expansion of the condensate width versus time at modulation parameter $K_0 = 2.4$ corresponding to the first zero of the Bessel function, is plotted in Fig. 2(a). The corresponding condensate image is in Fig. 2(c). The

dynamical localization leads to a blocking of the condensate expansion. By varying the optical lattice depth V_0 and the shaking frequency ω we verified that the universal behavior of $|J_{\rm eff}/J|$ was in very good agreement with the zero-order Bessel function rescaling of Eq. (19) for K_0 up to 6.

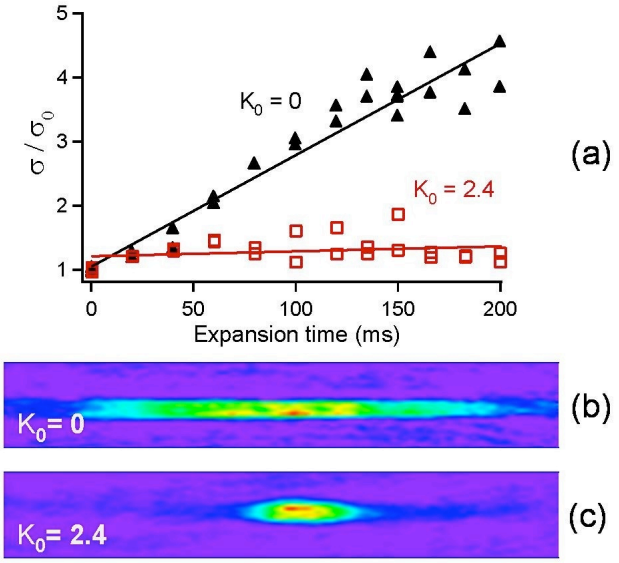

FIG. 2: Results for the free expansion of the condensate, measured in situ. In (a) plot of the condensate width versus versus expansion time at $K_0 = 0$ (open square) and $K_0 = 2.4$ (closed square) at $V_0 = 6E_{\rm rec}$. The straight lines fitted through the data allowed us to derive a reduction of the tunneling by a factor around 25. In (b) and (c) images at expansion time t =ms in a $V_0 = E_{\rm rec}$ lattice, for different values of the shaking parameter, $K_0 = 0$ and $K_0 = 2.4$ respectively.

Within the range $2.4 < K_0 < 5.5$ the zero-order Bessel function changes its sign, and also the tunneling rate. We verified this sign change by monitoring the phase coherence of the BEC in the shaken lattice, which was made visible by switching off the dipole trap and lattice beams and letting the BEC fall under gravity for 20 ms. The resulting spatial interference pattern is a series of regularly spaced peaks at $2n \times p_{\rm rec}$ with n integer (positive or negative), corresponding to the various diffraction orders of the propagating matter waves. A standard interference pattern, as corresponding to the J value of the tunneling rate at $K_0 = 0$, is presented in Fig. 3(a) with the maximum at $p = 0$ and two secondary maxima at $p = \pm 2p_{\rm rec}$. Such a pattern may be interpreted as the multiple source interference of Bloch waves with quasi-momentum $q = 0$ extending over the whole optical lattice. In the region between the first two zeros of the Bessel function, where $J_{\rm eff} < 0$, we found a typical interference pattern as in Fig. 3(c). That interference pattern is produced by a staggered Bloch wavefunction with $q = \pm k_{\rm L}$, at the edge of the Brillouin zone [37]. This different condensate wavefunction is produced by the inversion of the curvature of the (quasi)energy band at the center of the Brillouin zone when the effective tunneling parameter is negative, with energy minimum at the Brillouin zone edge, as plotted in Fig. 3(d).

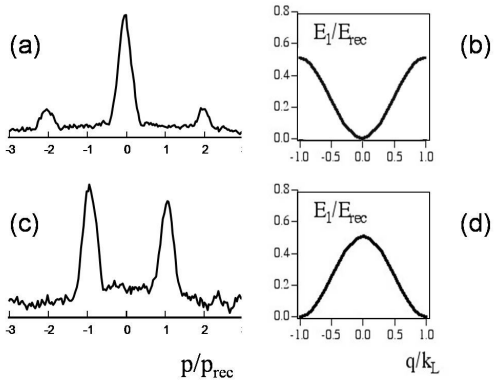

FIG. 3: In (a) and (c) interference of dressed matter waves released from an optical lattice with $V_0 = 9E_{\rm rec}$ and $\omega/2\pi =$ 3 kHz. The interference was measured by switching off the dipole trap and lattice beams and letting the BEC fall under gravity for 20 ms. In (a), interference at $K_0 = 1.5$, corresponding to $J_{\rm eff}/J = 0.51$; in (c), $K_0 = 3$ corresponding to $J_{\rm eff}/J = -0.26$. In (b) and (d) calculated ground energy band structure $E_1(q)$ versus the quasimomentum q for the corresponding values of V_0 and K_0.

In [22] we realized the coherent control of the dressed matter waves. Thus we changed adiabatically and reversibly the quantum state of ultracold bosons in driven optical lattices between a superfluid and a Mott insulator (MI) by varying the amplitude K_0 of the shaking. Within the Bose-Hubbard model described by the J and U parameters, if $U/J << 1$ the tunneling dominates and the atoms are delocalized over the optical latice. Instead for $U/J >> 1$ the interaction term leads to a loss of phase coherence through the formation of number squeezed states with increased quantum phase fluctuations. At a critical value of U/J the system undergoes a quantum phase transition to a MI state [38]. Using optical lattices one can tune U/J by changing the lattice depth, which affects both U and J through the width of the on-site wave functions. In addition at fixed lattice depth U can be increased making use of a Feshbach resonance. Alternatively we have suppressed J by periodically shaking the lattice and verified that the MI state is reached for a critical value of $U/J_{\rm eff}$.

In order to realize the driving-induced superfluid-MI transition, we first loaded a BEC into a 3D lattice with $V_0 = 11E_{\rm rec}$ using an exponential ramp of 150 ms duration and then linearly increased K_0 from 0 to $K_0 = 1.62$ in 4 ms, as schematized in the lower part of Fig. 4. While in an undriven lattice with at $11E_{\rm rec}$ lattice depth the BEC is superfluid with $U/6J = 3.5$, as shown by the interference pattern in the top lef of Fig. 4, for the driven lattice at $K_0 = 1.62$, $U/6J_{\rm eff} = 7.9$, *i.e.*, larger than the MI transition critical value. The distinct loss of phase coherence observed into the interference pattern on the

top right of Fig. 4 confirms that the system was in the Mott insulating phase, as in [38]. When K_0 was ramped back to 0, the interference pattern reappeared, proving that the transition was induced adiabatically and that the system was not excited by the driving.

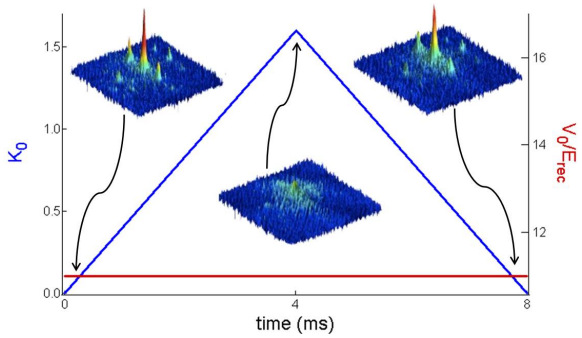

FIG. 4: Shaking-induced Mott insulator transition. (a) In a 3D lattice of constant depth ($V_0 = 11E_{\rm rec}$, as in the right scale) and driven at $\omega/2\pi = 6$ kHz, K_0 was ramped from 0 to $K_0 = 1.62$ in 4 ms and back, as schematized by the lines with the left scale. The interference patterns observed at $K_0 = 0$, at $K_0 = 1.62$ and back at $K_0 = 0$ are included.

In addition we compared the visibility of the interference pattern by inducing the MI transition in two different ways: (a) by increasing V_0 in an undriven lattice as in[38] and (b) by varying K_0 for constant V_0. The dependence of the visibility on $U/6J_{\rm eff}$ is the same for methods (a) and (b), strongly indicating that the same many-body state is reached by the conventional approach of increasing U or by our approach of keeping constant and reducing J through the dynamical localization.

VIII. CONCLUSIONS

Our results confirm and extend the role of cold atoms in optical lattices as versatile quantum simulators and open new avenues for the quantum control of cold atoms, thus establishing a link to coherent control in other systems such as Cooper pairs in Josephson qubits. The explored scenario is not intended as a look at the common superfluid-insulator transition from a different angle, but aims at obtaining genuinely new, nontrivial information on condensate dynamics. The control demonstrated here can be straightforwardly extended to more than one driving frequency and to more complicated lattice geometries such as superlattices [39]. In addition ref. [40] suggested that a control on the phase of the driving field may be used to produce and maintain a coherent atomic current. The application of dynamical localization to a triangular lattice Bose-Hubbard model allows the modeling of geometrically frustated antiferromagnetim [41].

IX. ACKNOWLEDGEMENT

Financial support by the EU-STREP NAMEQUAM and by a CNISM Progetto Innesco 2007 is gratefully acknowledged. We thank J. Radogostowicz and Y. Singh for assistance and A. Eckardt and M. Holthaus for the helpful suggestions. On of the authors (EA) thanks V.V. Konotop and M. Salerno for discussions.

[1] I. Bloch, J. Phys. B: At. Mol. Opt. Phys. **38** S629 (2005).
[2] O. Morsch and M. Oberthaler, Rev. Mod. Phys. **78**, 179 (2006).
[3] A. Eckardt and M. Holthaus, J. Phys.: Conference Series, **99**, 012007 (2008).
[4] R.E. Merrifield, J. Chem. Phys. **28**, 647 (1958).
[5] D.H. Dunlap and V.M. Krenke, Phys. Rev. B **34**, 3625 (1986).
[6] M. Holthaus, Phys. Rev. Lett. **69**, 351 (1992).
[7] M. J. Zhu, X.-G. Zhao, and Q. Niu, J. Phys.: Condens. Matter **11**, 4527 (1999).
[8] F. Grossmann, P. Jung, T. Dittrich, and P. Hänggi, Z. Phys. B **84**, 315 (1991).
[9] M. Grifoni and P. Hänggi, Phys. Rep. **304**, 229 (1998).
[10] E. Kierig, U. Schnorrberger, A. Schietinger, J. Tomkovic, and M. K. Oberthaler, Phys. Rev. Lett. **100**, 190405 (2008).
[11] Y. Kayanuma and K. Saito, Phys. Rev. A **77** 010101(R) (2008).
[12] C. Cohen-Tannoudji, Cargèse Lectures in Physics, vol. 2 M. Levy ed. (Gordon and Breach, 1968), p.347.
[13] S. Haroche, C. Cohen-Tannoudji, C. Audoin, and J. P. Schermann, Phys. Rev. Lett. **24**, 861 (1970).
[14] Q. Beaufils, T. Zanon, R. Chicireanu, B. Laburthe-Tolra, E. Marchal, L. Vernac, J.-C. Keller, and O. Gorceix, Phys. Rev. A **78**, 051603(R) (2008).
[15] K. W. Madison, M. C. Fischer, R. B. Diener, Q. Niu, and M. G. Raizen, Phys. Rev. Lett. **81**, (1998).
[16] R. Dum, A. Sanpera, and K.-A. Suominen, M. Brewczyk, M. Kuś, K. Rzążewski, and M. Lewenstein, Phys. Rev. Lett. **80**, 3899 (1998).
[17] M. M. Dignam and C. M. de Sterke, Phys. Rev. Lett. **88**, 046806 (2002).
[18] S. Longhi, M. Marangoni, M. Lobino, R. Ramponi, P. Laporta, E. Cianci and V. Foglietti Phys. Rev. Lett. **96**, 243901 (2006).
[19] R. Iyer, J. S. Aitchison, J. Wan, M. M. Dignam, and C. M. de Sterke, Opt. Expr. **15**, 3212 (2007).
[20] Yu. V. Bludov, V. V. Konotop, M. Salerno, arXiv:0907.3672v1, in press EPL
[21] H. Lignier, C. Sias, D. Ciampini, Y. Singh, A. Zenesini, O. Morsch, and E. Arimondo, Phys. Rev. Lett. **99**, 220403 (2007)
[22] A. Zenesini, H. Lignier, D. Ciampini, O. Morsch, and E. Arimondo, Phys. Rev. Lett. **102**, 100403 (2009).
[23] M. Cristiani, O. Morsch, J. H. Müller, D. Ciampini, and E. Arimondo, Phys. Rev. A **65**, 063612 (2002).
[24] R. Grimm, M. Weidemüller, and Y. B. Ovchinnikov, Adv. At. Mol. Opt. Phys. **42**, 95 (2000).
[25] N. Ashcroft and N. Mermin, Solid state physics, (Saun-

ders College, 1976).
[26] C. Kittel, Introduction to solid state physics, (John Wiley and Sons, 1996).
[27] W. Zwerger, J. Opt. B: Quantum Semiclass. Opt., **5**, S9 (2003).
[28] S. Raghavan, V. M. Kenkre, D. H. Dunlap, A. R. Bishop, and M. I. Salkola, Phys. Rev. A **54**, R1781 (1996).
[29] D. Jaksch, C. Bruder, J. Cirac, C. Gardiner, and P. Zoller, Phys. Rev. Lett. **81**, 3108 (1998).
[30] J. Shirley, Phys. Rev. B **138** 979, (1965).
[31] A. Eckardt, M. Holthaus, H. Lignier, A. Zenesini, D. Ciampini, O. Morsch, and E. Arimondo, Phys. Rev. A **79**, 013611 (2009).
[32] A. Eckardt, C. Weiss, and M. Holthaus, Phys. Rev. Lett. **95**, 260404 (2005).
[33] C. E. Creffield and T. S. Monteiro, Phys. Rev. Lett. **96**, 210403 (2006).
[34] A. Eckardt, T. Jinasundera, C. Weiss, and M. Holthaus, Phys. Rev. Lett. **95** 200401(2005).
[35] C. Sias, H. Lignier, Y. P. Singh, A. Zenesini, D. Ciampini, O. Morsch, and E. Arimondo, Phys. Rev. Lett. **100**, 040404 (2008).
[36] V. V. Ivanov, A. Alberti, M. Schioppo, G. Ferrari, M. L. C. M. Artoni, and G. M. Tino, Phys. Rev. Lett. **100**, 043602, (2008).
[37] R.G. Scott, A.M. Martin, S. Bujkiewicz, T.M. Fromhold, N. Malossi, O. Morsch, M. Cristiani, and E. Arimondo, Phys. Rev. A **69**, 033605 (2004).
[38] M. Greiner, O. Mandel, T. Esslinger, T.W. Hänsch, and I. Bloch, Nature (London) **415**, 39 (2002).
[39] C. E. Creffield, Phys. Rev. Lett. **99**, 110501 (2007).
[40] C. E. Creffield and F. Sols, Phys. Rev. Lett. **100**, 250402 (2008).
[41] A. Eckardt, P. Hauke, P. Soltan-Panahi, C. Becker, K. Sengstock, and M. Lewenstein, arXiv:09097.0423.